water

MDPI

Article

Impacts of Remedial Techniques on Contamination Transport in Groundwater

Walid M. A. Khalifa [1,2,*], Belkacem Achour [1], Tayyab Butt [1], Cyrus Raza Mirza [1], Heba Salah [3] and Sherif M. El-Didy [4]

[1] Civil Engineering Department, Faculty of Engineering, Ha'il University, Ha'il 81451, Saudi Arabia; b.achour@uoh.edu.sa (B.A.); ta.butt@uoh.edu.sa (T.B.); cy.mirza@uoh.edu.sa (C.R.M.)
[2] Civil Engineering Department, Faculty of Engineering, Fayoum University, Fayoum 63514, Egypt
[3] Khatib & Alami Office, El Tayaran St, Al Manteqah Al Oula, Nasr City, Cairo 11371, Egypt; hipamh@gmail.com
[4] Department of Irrigation and Hydraulics, Faculty of Engineering, Cairo University, Giza 12613, Egypt; smadidy@hotmail.com
* Correspondence: w.khalifa@uoh.edu.sa; Tel.: +966-504322771

Abstract: The significance of groundwater is largely shaped by the quality of wastewater from industrial, agricultural, and municipal sources. Understanding the controlling factors is essential to prevent the spread of contamination in groundwater. These factors could be divided into physical defenses, such as grouting and slurry walls, and hydrodynamic factors, such as injection and pumping wells. In this study, the groundwater transport model (MT3D) and the flow model (MODFLOW) were used to simulate four scenarios for groundwater protection. The first and second scenarios involve grouting and constructing slurry walls to change their depth, permeability, and thickness. The third and fourth scenarios involve injection and pumping wells changing the rate of flow, screen length, and the number of wells. The results show that increasing the thickness of the grouted soil and increasing the grouting depth help to control the level of contamination. Furthermore, multi-slurry walls upstream or downstream of the contamination source are sufficient for preventing the spread of contaminants. The results also reveal that rising rates of injection or pumping wells allow for minimal contamination propagation. The growing number of wells provided greater control over the injection rather than pumping wells. The variation in the screen length of pumping wells is effective for preventing the propagation of contamination.

Keywords: groundwater; contamination transport; grouting/slurry walls; injection/pumping wells; numerical models

check for updates

Citation: Khalifa, W.M.A.; Achour, B.; Butt, T.; Mirza, C.R.; Salah, H.; El-Didy, S.M. Impacts of Remedial Techniques on Contamination Transport in Groundwater. *Water* **2024**, *16*, 3277. https://doi.org/10.3390/w16223277

Academic Editor: Constantinos V. Chrysikopoulos

Received: 18 September 2024
Revised: 1 November 2024
Accepted: 5 November 2024
Published: 14 November 2024

1. Introduction

Groundwater represents about 97% of the freshwater around the world [1,2]. Hence, it is the predominant and most frequently used water resource for humans both in the present and in the future. Anthropogenic activities are considered to be the main causes of the deterioration in groundwater quality [3]. As such, sustainably managing and ensuring the quality of groundwater are extremely challenging [4,5]. Various remediation processes can be used to treat contaminated groundwater. These include slurry walls, injection, and pumping. Grouting includes a low viscous injection into the voids of granulated soils. There are several factors that can affect the design of grouting, such as the material, grouting size, the relative density and fine contents of soil, the water–cement ratio of grout mixture, and grouting pressure. The best application of grouting is in deep vadose, which can limit the water flux in contaminated zones. However, grouting can be beneficial when used in conjunction with other techniques [6]. In some industrial areas, which face significant contamination, a technique of jet grouting with exchange reagents which can strongly mix with the contaminants was proposed [7]. This technique enables investigating a zone of highly contaminated subsoil before and after the treatment, with measurements directly showing the success of the dechlorination process. A simulation was performed to investigate the role of the thermal and hydraulic conductivities of the grout when the borehole heat exchangers enhance the effects of significant groundwater flow [8].

Vertical barriers, including slurry trench walls and walls constructed with soil mix technology, have been employed for decades to control groundwater flow and subsurface contaminant transport. Slurry walls are used to divert the flow of uncontaminated groundwater and/or provide a hindrance for groundwater treatment [9–13]. Amended calcium bentonite was proposed for use in backfills for slurry trench cut-off walls for the containment of lead contamination in groundwater [9]. This technique decreases the hydraulic conductivity of the backfill to nearly 2×10^{-10} m/s. The authors of [10] presented a framework for evaluating a containment system involving barriers such as slurry walls and jet grouting or hydraulic methods such as pumped-treated wells according to capital and operational costs. The contaminant mass discharge from the containment system is a robust indicator of its effectiveness and can be derived from modeling results. Several experiments have been conducted to investigate the engineering characteristics of soil–cement–bentonite (SCB) backfill [13]. The results indicate that the water content in the slurry is more sensitive to the bentonite content. Further, the unconfined compression strength (UCS) value increased with the cement content. The permeability coefficient decreased drastically as a result of increases in the cement and bentonite contents.

The systems of injection wells or pumping wells are considered to be effective methods to prevent the dispersion of contaminants [14–16]. An investigation [14] considered a sulfate-contaminated site in China as the research objective. A hydraulic barrier was created to cut off the pollution sources. Another hydraulic technique used involved boring nine holes to control the pumping wells, which were arranged in the polluted area, and injection wells, which were arranged at the outer edge of the pollution region, so that the zone of the pollution plume was gradually reduced. After two years of continuous monitoring, the sulfate concentrations decreased in the monitoring wells, indicating that integrated groundwater remediation techniques are more effective and more reliable than one single technique.

A comparison between pump-and-treat (P and T) and groundwater circulation wells (GCW) was drawn in a study [16], which focused on two industrial sites. The comparative assessment was based on the mobilization patterns observed, the resulting variations in contaminant concentration, the mass discharge, and the volume of extracted groundwater. One conventional well mobilized higher masses of contaminants in the early stages of P and T. This reflected P and T's impact on accessible contaminant pools in early operational periods. P and T withdraws a significantly larger volume of groundwater than the GCW. GCWs have been shown to reduce remediation time, increase mass removal, and minimize the significant water consumption associated with P and T.

The contamination process of the groundwater from drains and canals was studied using a coupled model of MODFLOW and MT3DMS [17]. The authors applied their study findings to two cases, one hypothetical and one real, involving the Nile Delta Aquifer (NDA). The study presented four different scenarios. The first involved changing polluted drain and canal boundary conditions such as the head and concentration by identifying groundwater contamination as total dissolved solids (TDSs). The second studied the source of polluted drain in a low-permeability layer or a confined aquifer. The third was based on installing a cut-off wall in the polluted drain sides. The fourth investigated the lining of polluted drains. The results revealed that aquifer contamination was decreased by increasing the water head of canals by 50 cm and decreasing the drain head by 50 cm and the concentration by 25%. For the hypothetical case, contamination was decreased by providing a clay cap, which reduced the aquifer's hydraulic conductivity. Further, the results showed the effectiveness of using a cut-off in shallow aquifers (hypothetical case), in which the aquifer salt was reduced by nearly 30%. In the case of drain linings, the aquifer salt concentration reduced to low levels in hypothetical and real cases, indicating that this case is more efficient in controlling groundwater contamination.

The rates and numbers of injection/pumping wells can minimize the contamination by choosing the appropriate well location and the space between wells [18]. In another study [19], the remedial and economic efficiency of a recirculation well system with sinusoidal temporally varying pumping and injection rates was evaluated for enhancing remediation. They performed sensitivity analyses to determine the optimal values of four operational parameters associated with the effects of temporally variable pumping or injection rates on the cumulative swept area of injected chemical amendment for a given operation time or cumulative injected volume, which are good measures of remediation and economic efficiency. Another study based on 3D model to simulate unsteady and spatially varying groundwater flow, along with contaminant migration, was conducted, which was capable of investigating well water quality based on the change in the wells' pumping rates. The modeling results revealed that choosing an optimum range for the pumping rate increases contaminant travel time and reduces aquifer vulnerability [20].

In the current study, some remedial techniques such as grouting, slurry walls, and injection/pumping wells are implemented and discussed using the integrated numerical programs of the contaminants transport (MT3D) and hydraulics (MOFDLOW). Changes in grouting depth, permeability, thickness, and slurry wall's location are considered. Further, variations in injection/pumping rate, screen posture, and well allocation around the contamination provenance are considered.

2. Materials and Methods

2.1. Coupled Hydrodynamic and Transport Models

In this study, the hydrodynamic model (MODFLOW) is combined with the transport model (MT3D). The MT3D model can be deemed as 2D or 3D for simulation of the groundwater contaminants through advection, dispersion, and chemical reactions [21,22]. MT3D uses MODFLOW to restore the hydraulic heads and the diverse flow and source/sink terms [23–27]. The transport equation of MT3D in a porous medium includes the dispersion coefficient (longitudinally and transversely) and the effective porosity [28–32]. The equation of the used groundwater flow in MODFLOW [23] is as follows:

$$\frac{\partial}{\partial t}\left(K_{xx}\frac{\partial h}{\partial x}\right)+\frac{\partial}{\partial y}\left(K_{yy}\frac{\partial h}{\partial y}\right)+\frac{\partial}{\partial z}\left(K_{zz}\frac{\partial h}{\partial z}\right)+W=S_s\frac{\partial h}{\partial t} \quad (1)$$

The equation of the transport model MT3D [27] is as follows:

$$\frac{\partial C}{\partial t}=\frac{\partial}{\partial xi}\left(D_{ij}\frac{\partial C}{\partial xj}\right)+\frac{\partial}{\partial xi}(V_iC)+\frac{q_s}{\theta}(C_s)+\sum_{k=1}^{N}(R_K) \quad (2)$$

where K_{xx}, K_{yy}, and K_{zz} represent the conductivity of the aquifer along the x, y and z axes ($L.T^{-1}$); h is the flow head (L); W represents the sources/sinks of water (T^{-1}); S_s is the specific storage (L^{-1}); t is the time (T); C is the concentration of groundwater (ML^{-3}); D_{ij} is the dispersion tensor ($L^2.T^{-1}$); i, j represent the cell indices; V_i is the seepage velocity ($L.T^{-1}$); q_s is the water flux (positive) as sources and (negative) as sinks (T^{-1}); θ is the porosity (dimensionless); C_s is the concentration of sources or sinks ($M.L^{-3}$); R_K is the rate of solute production or decay in reaction k of N different reactions ($M.L^{-3}.T^{-1}$).

2.2. Hypothetical Study Zone and Boundary Conditions

The numerical models MODFLOW and MT3D were applied in the suggested hypothetical study zone using the square shaped with a net-of-cells grid (100 × 100). Each cell is 8 × 8 m^2 representing a whole area 800 × 800 m^2. The aquifer has a depth of 30 m. The aquifer has four layers (5, 5, 10, and 10 m) downwardly. Figure 1 shows a finite difference grid of the study zone. Each layer has a hydraulic conductivity of 10 $m.d^{-1}$ and porosity 0.3. The dispersion coefficient is taken as 500 m [33]. The specified boundaries are taken 29 m (west) and 26 m (east) according to the groundwater flow direction. Some substances found naturally in rocks or soils, such as iron, manganese, arsenic, chlorides, fluorides, sulfates, or radionuclides, can become dissolved in groundwater. The source of contaminant is given at the crossing cell of row #49 (Y = 392 m) and column #28 (X = 224 m). The source concentration is assumed to be 300 ppm. Figure 2 shows a horizontal view and cross-section A-A of the equipotential heads and velocity vectors of the study zone.

(**a**)

(**b**)

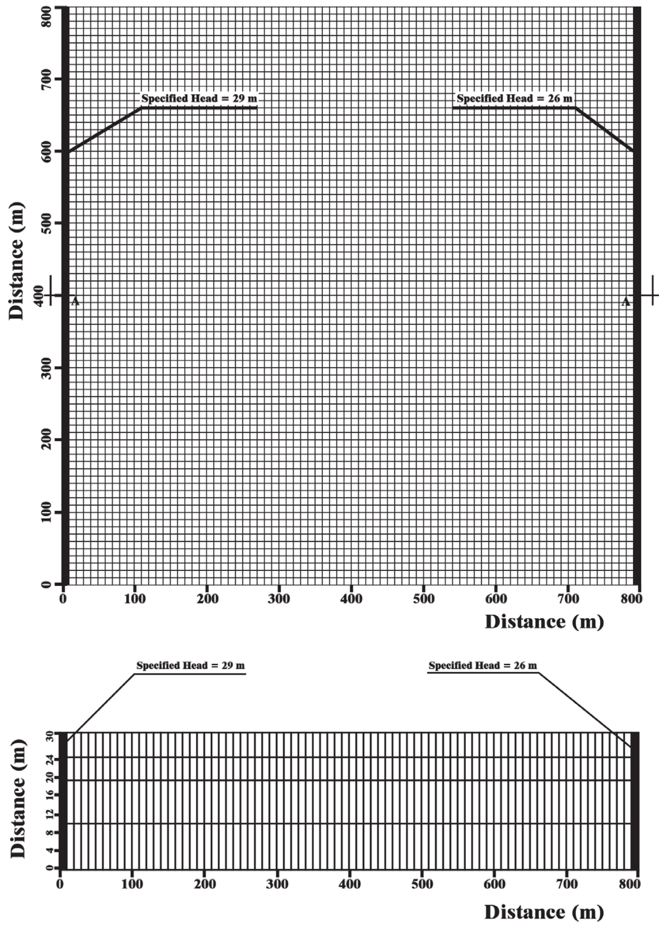

Figure 1. (**a**) Plan of the three-dimensional finite difference grid, (**b**) cross section A-A of four layers.

(**a**)

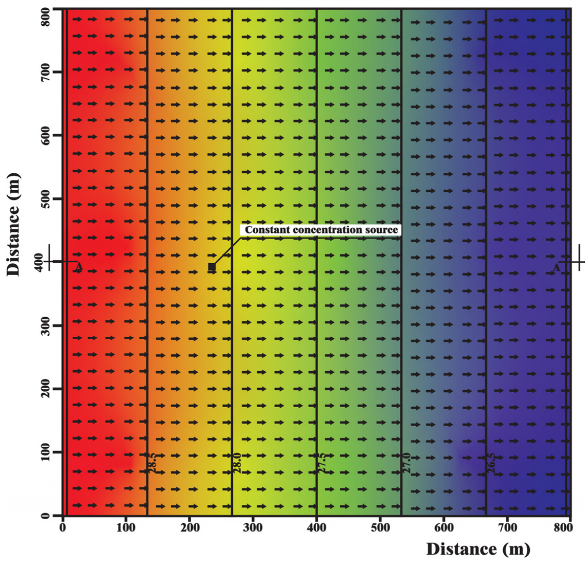

Figure 2. *Cont.*

(**b**)

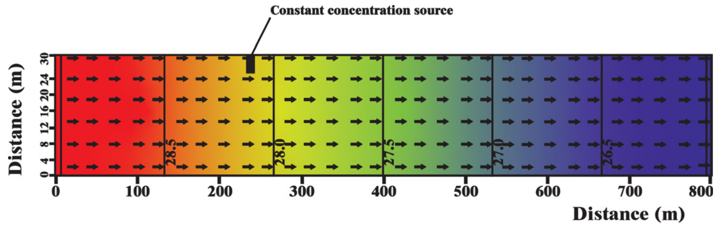

Figure 2. (**a**) A horizontal view of equipotential heads and velocity vectors, (**b**) a corresponding cross-section A-A of the equipotential heads and the velocity vectors.

Calibration of the Used Model

The authors [34] calibrated the used model using seven monitoring piezometers as shown in Figure 3. The head of the injection well was set 5.0 m above the static water level of the groundwater. The chloride injection rate was 5.00 $m^3.d^{-1}$. After the injection started, the samples of water were taken periodically over 4 h from all piezometers. The primary injection concentration of chloride was 1400 ppm in the groundwater. Table 1 shows the distribution of monitoring piezometer locations from an injection well. The results were obtained by trial and error. The root mean squared (RMS) was 1.025 m with normalized RMS of 30.138%; the maximum and minimum residuals were −1.095 m and +0.914 m with mean residual −0.413 m. The absolute residual mean was 1.022 m.

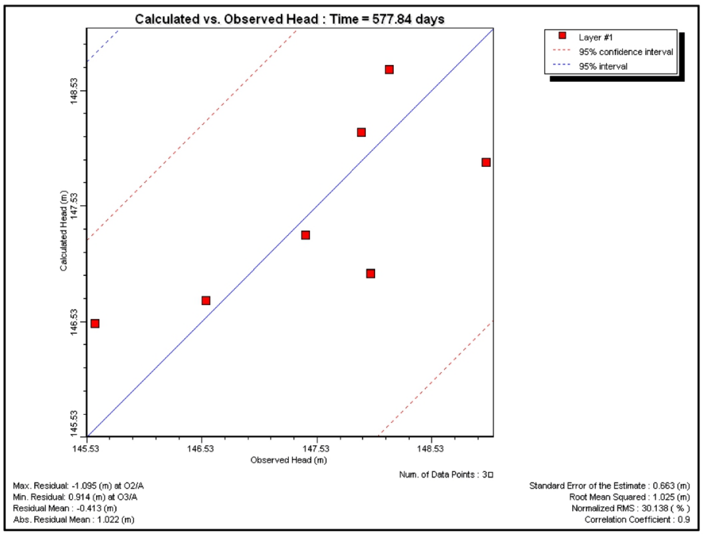

Figure 3. Model calibration results [34].

Table 1. Location of monitoring piezometers.

Piezometer	1	2	3	4	5	6	7
Distance (m)	11	11.5	24.8	38.6	51.5	62.3	70.4

2.3. Types of Groundwater Remediations

Four types of groundwater remediation are suggested. These remediation measures are demonstrated, discussed, and presented. The studied measures are grouting, slurry walls, injection wells, in addition to contaminant withdrawal by pumping wells acting as interceptors.

2.3.1. Grouting

The grouting material fills the soil pores and reduces the hydraulic conductivity. Creating a grouting curtain around the contamination source acts as a low-permeability barrier that prevents the contamination spread in the aquifer domain. Investigation of the effect of depth, permeability, and thickness of the grouting curtain is presented.

2.3.2. Slurry Wall

There is no big difference between the function of the slurry walls and the grouted soil. Both behave in the same way by reducing the hydraulic gradient and the velocity vectors through the soil pores, preventing contaminant transfer from one place to another. The simulation of the slurry wall presented three scenarios: a straight slurry wall upstream of contamination source, three-sided confining slurry wall upstream and downstream of contamination source.

2.3.3. Injection Wells

In this study, three scenarios of injection wells are suggested. These types of injection wells depend on the rate, the depth of the screen, and the number of injection wells. We present their effect on the spread of contaminants.

2.3.4. Pumping Wells

The fourth technique for groundwater remediation is withdrawal via pumping wells. The study scenarios in this section concern the pumping rate, screen depth, and well number.

3. Results and Discussion

This study focuses on groundwater remediation. The remediation proposed four patterns, such as grouting, slurry walls, injection wells, and pumping wells.

3.1. Grouting

The aim of the grouting process is to ameliorate the shear strength by growing the consistency of soil particles. This study introduces the effect of grouting depth, permeability, and grouting thickness on the contamination transport.

3.1.1. Effect of Grouting Depth

Partial Depth Grouting Zone

A grouted impermeable zone of thickness 8 m (one cell) is simulated around the contamination source, a region of 72 m by 72 m (nine cells by nine cells). If the grouted side walls of the box penetrate only the upper three layers without going through the fourth one, for that case, Figure 4 shows the velocity vectors and the equipotential lines. It is shown that the pattern of velocity vectors inside and then outside the box of grouting can convey the contamination outside the box, as shown in Figure 5. It gives a plan of the concentration lines after 300 days, where Figure 6 shows a vertical view of the concentration spread.

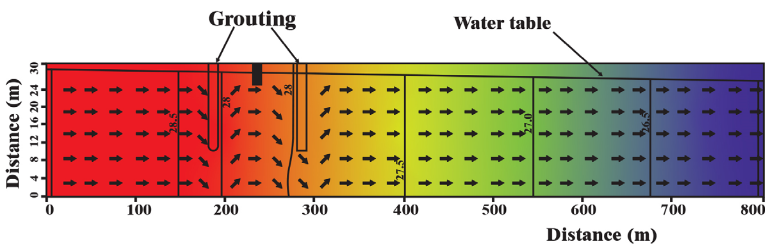

Figure 4. Equipotential lines and velocity values in a vertical section for grouting the thickness of one cell.

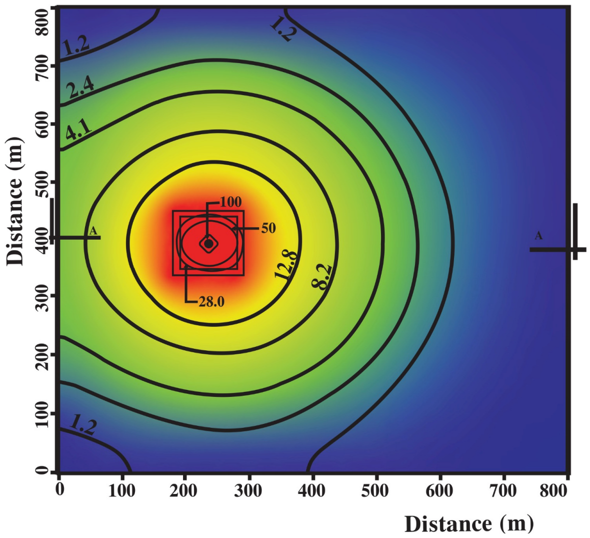

Figure 5. Concentration in a horizontal view for grouting of thickness one cell.

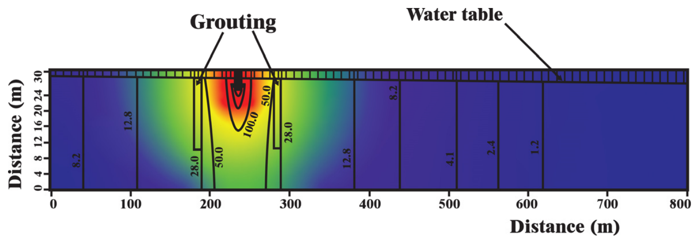

Figure 6. Concentration in a vertical section for grouting of thickness one cell.

Full-Depth Grouting Zone

The grouting curtain goes all the way to the aquifer bed, penetrating all the layers with the same conditions of the partial depth. Figures 7 and 8 show that the contamination is trapped inside the box whose side walls are grouted soil and bottom is the aquifer impermeable bed [35]. The grouted soil reduces the velocity entering or leaving the created box [36–39]. The contaminant remains in place inside the box and does not spread through the aquifer domain.

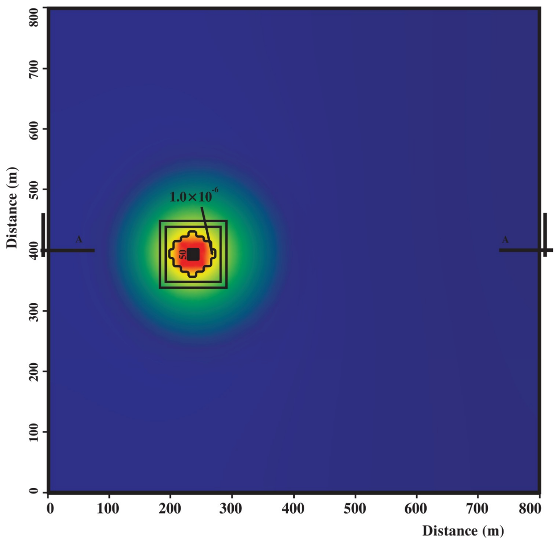

Figure 7. Contamination in a horizontal view is surrounded by full-depth grouting of thickness one cell.

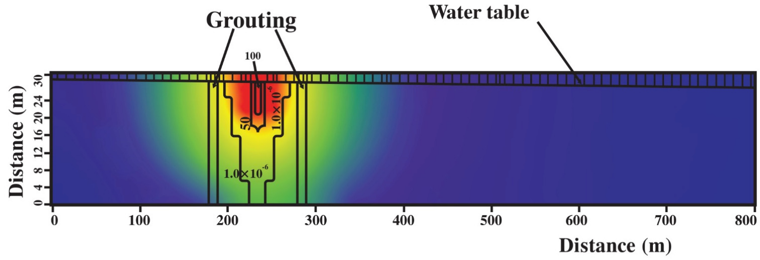

Figure 8. Contamination in a vertical view is surrounded by full-depth grouting of thickness one cell.

Figures 9 and 10 present the contamination concentration in the first and fourth layers, respectively, for the following cases: no grouting, grouting without reaching the aquifer bed, and grouting reaching the aquifer bed. Both layers become polluted when the grouting does not reach the aquifer bed. The grouting is not effective if it does not reach the aquifer bed [8,40–42].

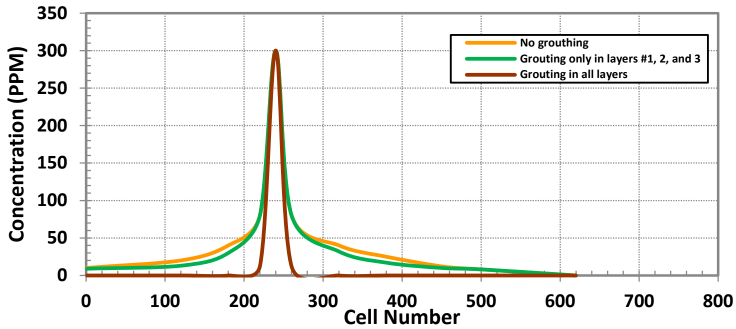

Figure 9. Grouting depth effect on a contaminant spread in layer #1.

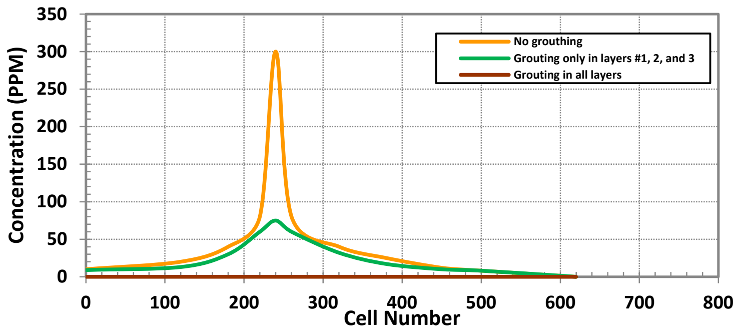

Figure 10. Grouting depth effect on a contaminant spread in layer #4.

3.1.2. Effect of Grouting Permeability

Figure 11 presents the concentration lines when assuming more permeability for the grouted soil (0.01 m/day). Permeability, which is much greater than the assumed one in Figures 7 and 8 (impermeable, 10^{-8} m/day), allows for contamination transfer outside the grouting box through the walls, as shown in Figures 11 and 12 [6,17,43,44].

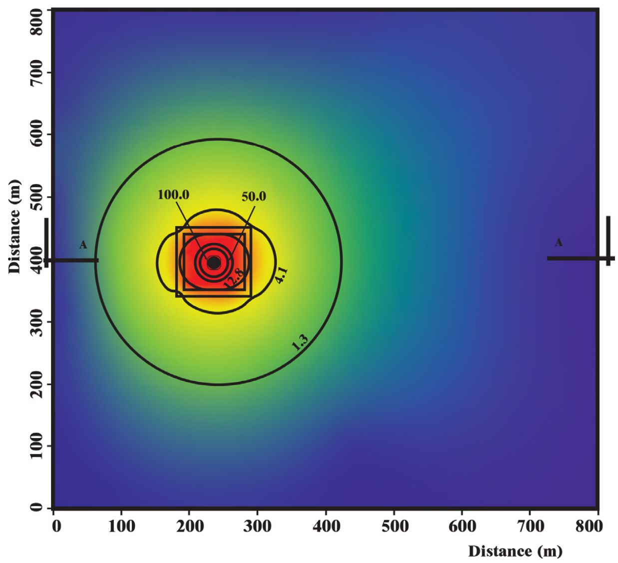

Figure 11. Concentration in a horizontal view for grouting of thickness one cell with conductivity 0.01 m/day.

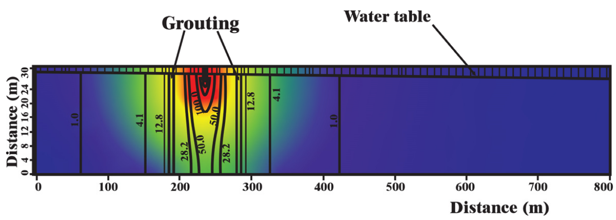

Figure 12. Concentration in a vertical section for grouting of thickness one cell with conductivity 0.01 m/day.

3.1.3. Effect of Grouting Thickness

The example of low grouting permeability (Section 3.1.2) is used here again but increasing the grouting thickness by as much as three times (24 m). A comparison of results in Figures 11 and 12 with Figures 13 and 14, respectively, reveals that increasing the thickness of the grouted soil reduces the transfer of the contamination outside the grouted box because it decreases the hydraulic gradient through the grouted soil [8,45].

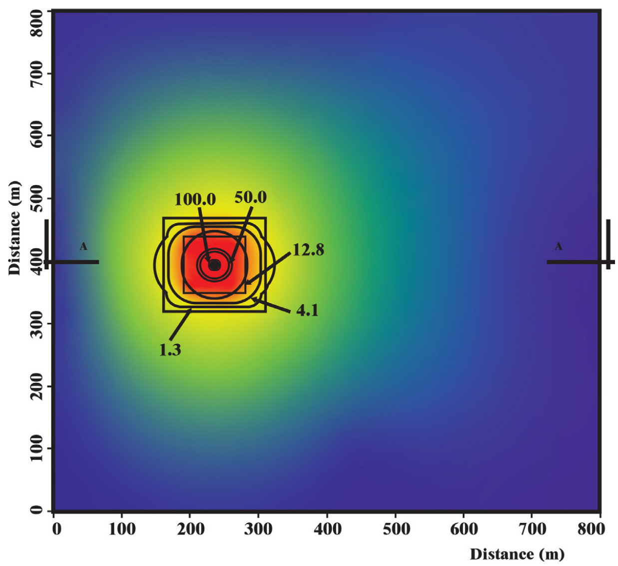

Figure 13. Concentration in a horizontal view for grouting of thickness three cells.

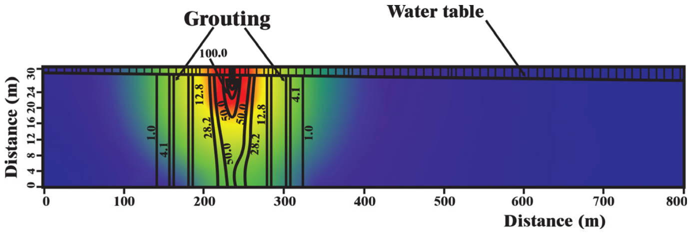

Figure 14. Concentration in a vertical section for grouting of thickness three cells.

3.1.4. Impact of Grouting Scenarios on Contamination Transport

A comparison between all grouting scenarios is summarized in Figure 15. In the figure, the worst condition is when the grouting depth is partial. Better conditions for controlling the contamination transport were the full grouting to the end of the aquifer with the minimum permeability and a thick grouting zone.

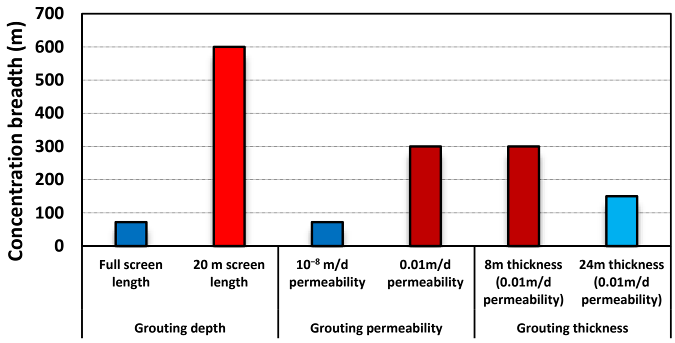

Figure 15. Effect of grouting factors on contamination spread.

3.2. Slurry Wall

The results of the parametric study for the grouting effect are applicable to the effect of the slurry wall. In the present section, the shape of the slurry wall around the contamination source is investigated after 300 days of its construction. The obtained results are also valid for the grouted soil. Simulation of a straight slurry wall upstream of the contamination source is not enough for preventing the contamination spread, as shown in Figure 16. Figures 17 and 18 show that having a three-sided confining slurry wall (or grouted soil) gives better results in trapping the contaminant in place and preventing its spread [10,46].

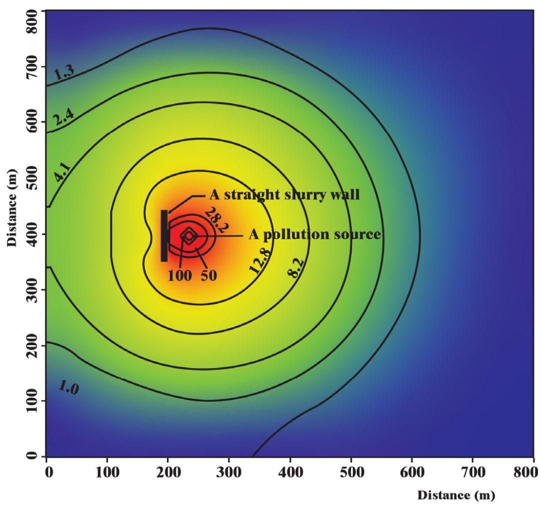

Figure 16. Concentration in a horizontal view for a straight slurry wall upstream a contamination source.

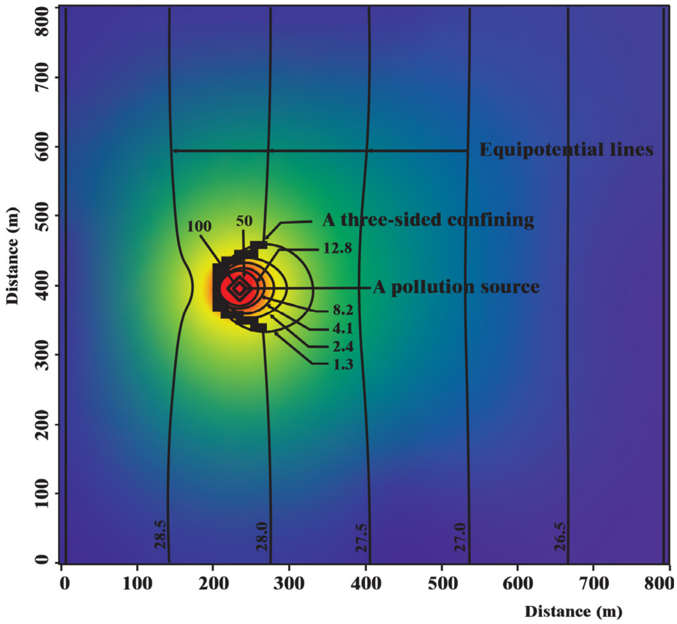

Figure 17. Concentration in a horizontal view for a three-sided confining slurry wall upstream a contamination source.

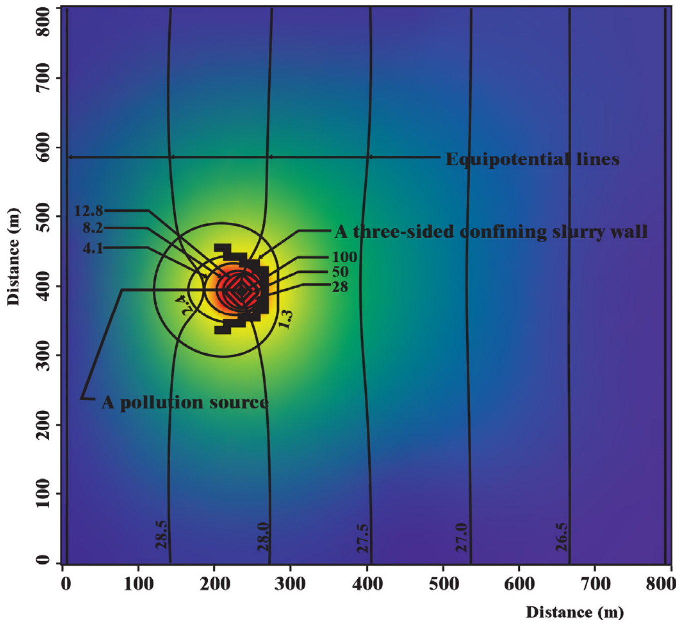

Figure 18. Concentration in a horizontal view for a three-sided confining slurry wall downstream of contamination source.

3.3. Injection Wells

This study presents three cases of injection wells of clean water. Theses statuses show the effect of injection rate, screen depth, and number of wells on the contamination transport.

3.3.1. Effect of Injection Well Rate

This study provides four-injection wells with clean water located around the contamination source as shown in Figure 19. In the four layers of the aquifer, the screen of the wells is completely penetrated. For each well, the injection rate is 600 $m^3.d^{-1}$. Figure 19 shows the restricted containment of the concentration spread (about 100 m wide). Figure 20 shows the spread of concentration for lowering the rate with 300 m^3.d^{-1}. In that case, more spread of contamination occurs (about 300 m wide) [19,47,48].

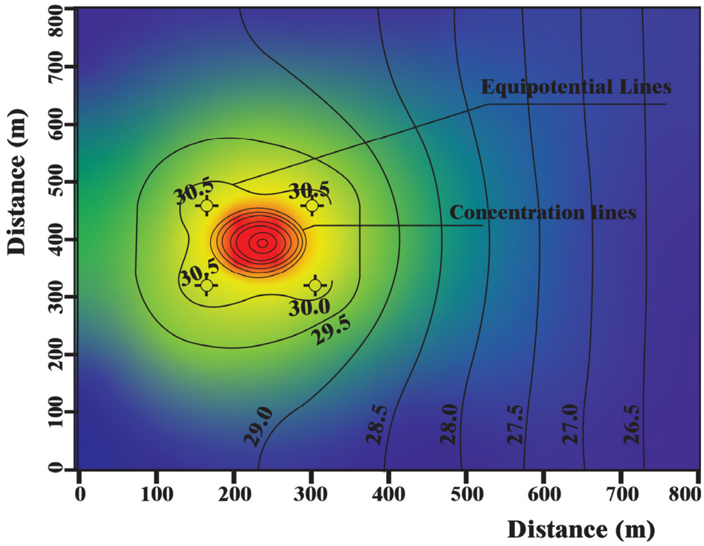

Figure 19. Contamination concentration spread for four-injection wells with rate 600 m^3.d^{-1}.

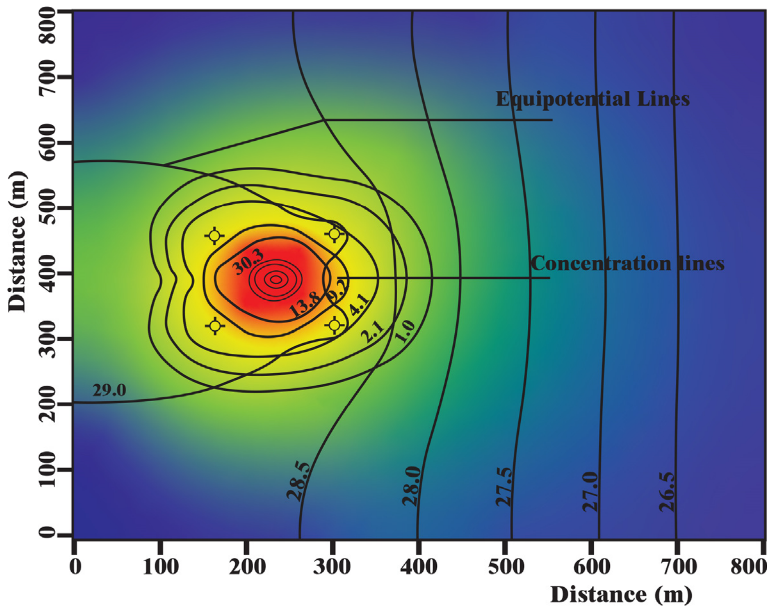

Figure 20. Contamination concentration spread for four-injection wells with rate 300 m^3.d^{-1}.

3.3.2. Effect of Screen Depth of Injection Wells

For the case of an injection rate of 300 m^3.d^{-1}, the screen length is taken as 10 m only in the lower part of the aquifer. Figure 21 shows the spread of concentration in the first layer. An insignificant rise in the contamination spread can be seen in Figure 20 [14,49].

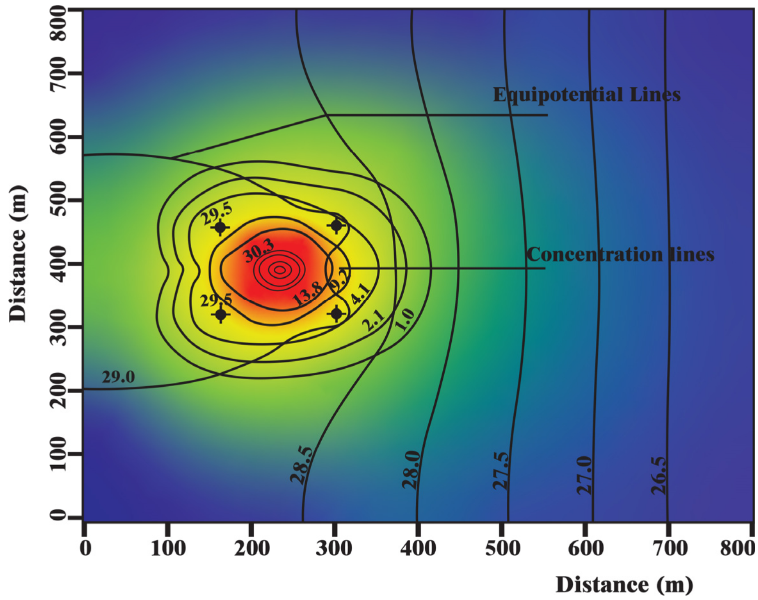

Figure 21. Contamination concentration spread for four-injection wells with rate 300 $m^3.d^{-1}$ and screen in the lower 10 m.

3.3.3. Effect of Injection Well Number

Referring to the case of Figure 19, the injection wells are reduced to two upstream. In this case, more contamination is noticed (around 400 m wide), as shown in Figure 22 [19].

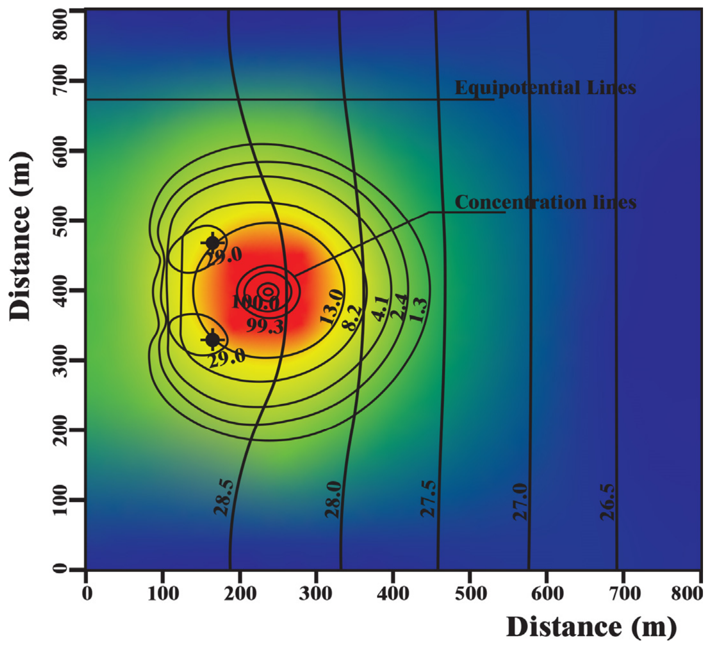

Figure 22. Contamination concentration spread for two-injection wells with rate 300 $m^3.d^{-1}$.

3.4. Pumping Wells

The pumping wells for withdrawal of the contamination aquifer represent the fourth technique of groundwater remediation. In this type of remediation, the effects of pumping rate, screen depth, and well numbers on the contamination transport are presented.

3.4.1. Effect of Pumping Well Rate

This study introduced four pumping wells, located as shown in Figure 23, to prevent contamination spreading through the aquifer. The wells have full screens to the last layer with a rate of 600 $m^3.d^{-1}$. Figure 23 displays contour lines of the head and concentration. In this case, the contamination area is confined among the four wells. In contrast, Figure 24 shows the contamination spreading out of the well zone with a rate of 300 $m^3.d^{-1}$. The reducing pumping rate was set earlier, as in [20].

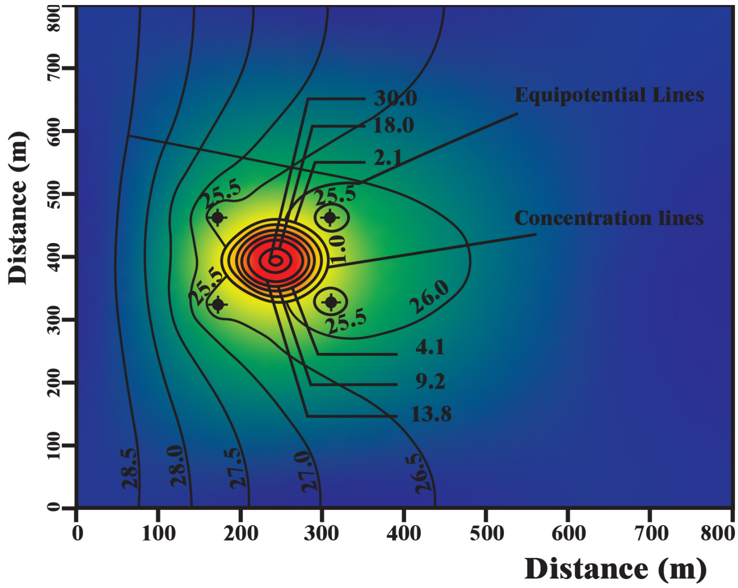

Figure 23. Contamination concentration spread for four-pumping wells with rate 600 $m^3.d^{-1}$.

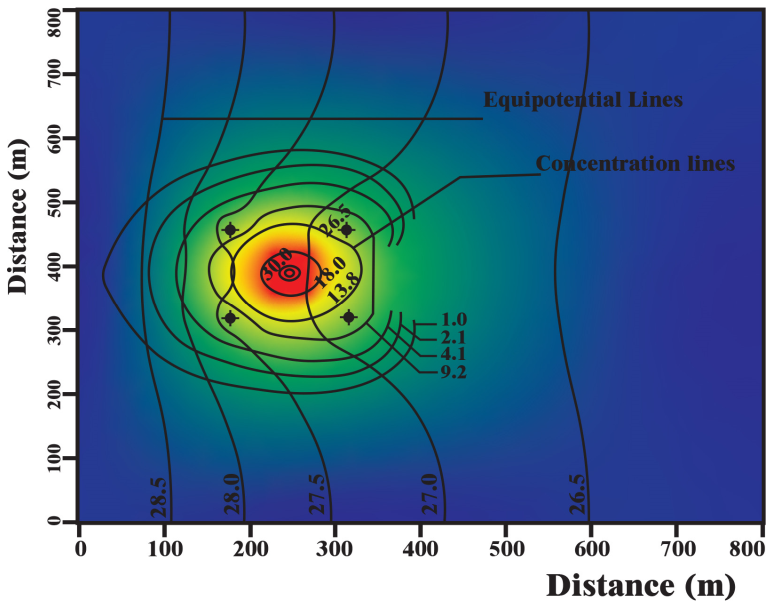

Figure 24. Contamination concentration spread for four-pumping wells with rate 300 $m^3.d^{-1}$.

3.4.2. Effect of Screen Depth of Pumping Wells

For the case of a pumping rate of 300 $m^3.d^{-1}$, the screen length was taken as 10 m only in the lower part of the aquifer. Figure 25 shows the spread of contamination in the first layer. This result shows more contamination other than that in Figure 24. This happens in the first layer when the discharging screen is far away from the fourth layer [50].

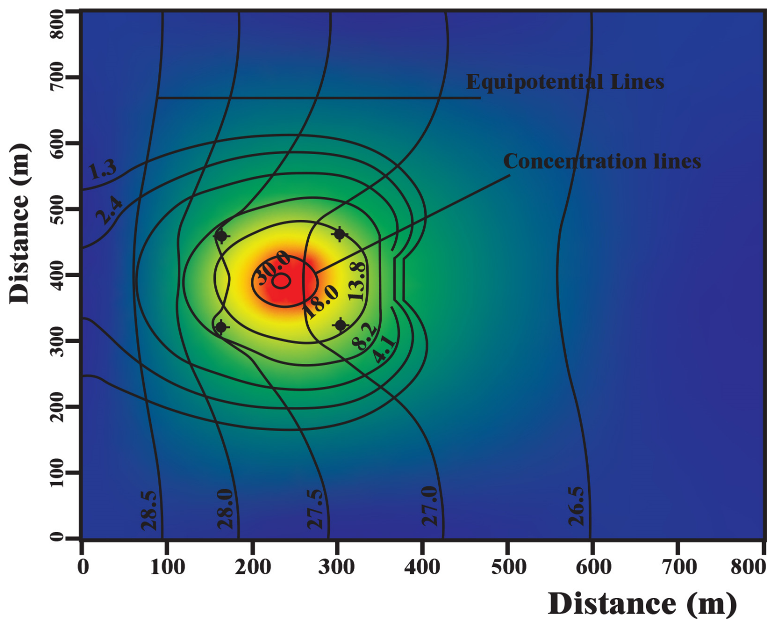

Figure 25. Contamination concentration spread for four-pumping wells with rate 300 $m^3.d^{-1}$ and screen in the lower 10 m.

3.4.3. Effect of Pumping Wells Number

Figures 26 and 27 show the effect of the reduction in the number of pumping wells. The contamination spread is increased compared with Figure 24 [20].

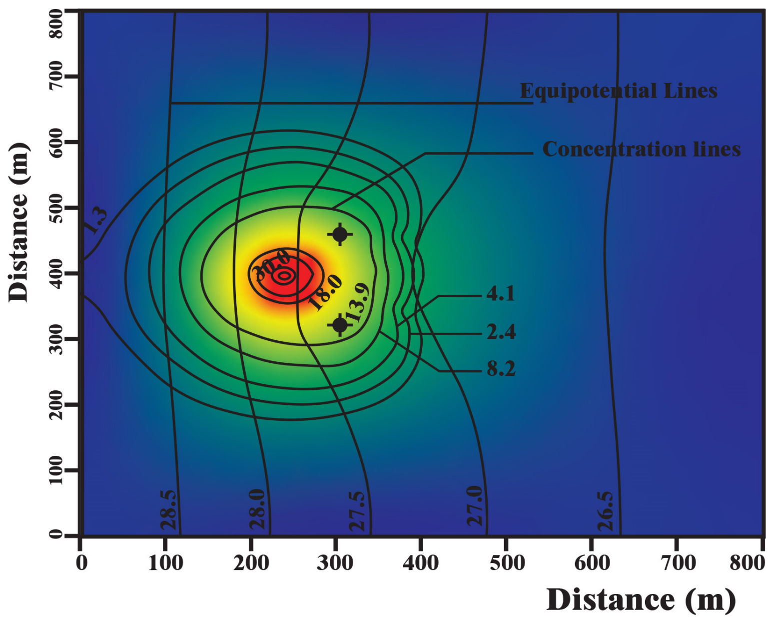

Figure 26. Contamination concentration spread for two-pumping wells of clean water with rate 300 $m^3.d^{-1}$.

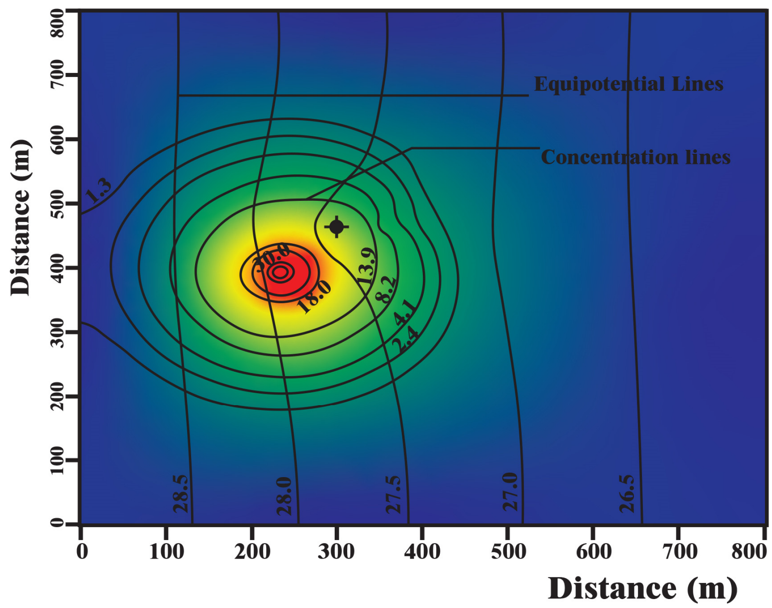

Figure 27. Contamination concentration spread for one-pumping wells of clean water with rate 300 $m^3.d^{-1}$.

3.5. Effect of Injection/Pumping Wells on Spread of Contamination

According to the change in flow rate, screen depth, and number of wells, Figure 28 shows the relationship of the contamination propagation over the contaminated zone. Based on the blue color for the injection wells and green color for the pumping wells, Figure 28 shows the spread of contamination that could be limited due to injection wells rather than pumping wells. In the figure, the total screen length seems a good option for reducing the contamination propagation, especially for pumping wells. Finally, the increasing number of wells for both injection and pumping wells played a significant role in reducing the contamination spread.

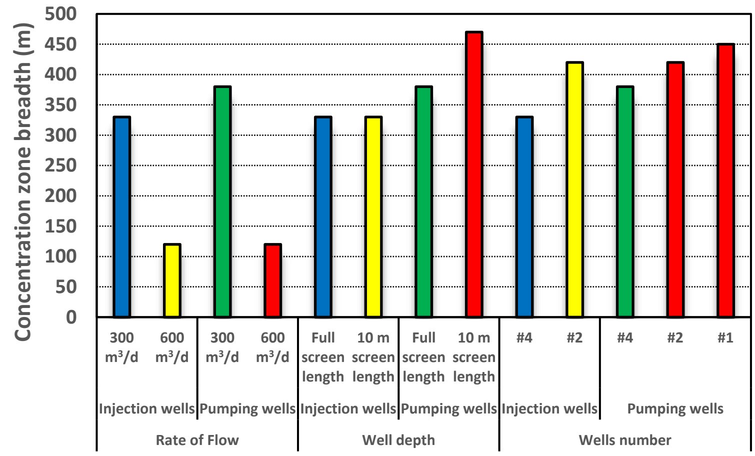

Figure 28. Effect of injection/pumping well factors on contamination spread.

4. Conclusions

The present study highlights the main factors that could control the three-dimensional spread of a contaminant in a porous medium. It helps explain the behavior of different remediation measures and the design of successful control systems. The major outcomes of this study are as follows:

- Grouting of soil creates a low-permeability medium that reduces the hydraulic gradient and the corresponding pore velocity preventing the spread of contaminants.

- Slurry walls act as low-permeability barriers that can confine contaminants and prevent their migration.
- Increasing the thickness of the grouted soil reduces the transfer of contamination through the grouted medium.
- The depth of grouting is an important factor to consider in the design of a confining system. Greater grouting depth improves control over the contaminant spread.
- One straight slurry wall upstream of the contamination source is insufficient in preventing contaminant spread.
- Higher clean water injection rates and pumping rates for hydrodynamic control allow for reduced contaminant spread.
- Increasing the injection well number and pumping wells reduces the spread of contaminants.
- Changing the screen length of the pumping wells is effective in controlling the contamination propagation.
- The effect of changing the screen length of the pumping wells on the contamination spread is more than that of injection wells.
- Changing the number of pumping wells has a greater effect on contaminant spread compared to a change in injection wells.

5. Recommendations

Out of this study, the following recommendations should be considered:

- Grouting should penetrate the whole aquifer thickness, reaching its impermeable bed to trap the contaminant in position.
- The permeability of grouted soil should be low enough to prevent the migration of a contaminant.
- The grouted soil should be thick enough to prevent contaminant penetration through the soil.
- More complete grouting around the contamination source helps in confining the contaminant position.
- All the above-mentioned factors are also applicable to slurry walls.
- The flow rate and well number for the injection/pumping method should be studied in detail when designing an effective system.

Author Contributions: Conceptualization, S.M.E.-D. and W.M.A.K.; methodology, H.S.; software, C.R.M.; validation, T.B., B.A. and W.M.A.K.; formal analysis, T.B. and W.M.A.K.; writing—original draft preparation, S.M.E.-D.; writing—review and editing, W.M.A.K. and T.B.; visualization, C.R.M.; supervision, W.M.A.K. and S.M.E.-D.; project administration, W.M.A.K.; funding acquisition, W.M.A.K. All authors have read and agreed to the published version of the manuscript.

Funding: This research was funded by the Scientific Research Deanship of the University of Ha'il, Saudi Arabia, through the project number RG-21168.

Data Availability Statement: Data availability is only for the calibration https://doi.org/10.1016/j.aej.2024.09.009.

Conflicts of Interest: The authors declare no conflicts of interest.

References

1. Babiker, I.S.; Mohamed, M.A.; Terao, H.; Kato, K.; Ohta, K. Assessment of groundwater contamination by nitrate leaching from intensive vegetable cultivation using geographical information system. *Environ. Int.* **2004**, *29*, 1009–1017. [CrossRef] [PubMed]
2. WHO. *Fluoride in Drinking Water, World Health Organization*; IWA Publishing: London, UK, 2006.
3. Chengcheng, X.; Guodong, L.; Hongye, X.; Fangting, J.; Yuchuan, M. Influence of saline intrusion on the wetland ecosystem revealed by isotopic and hydrochemical indicators in the Yellow River Delta. *China. Ecol. Indic.* **2021**, *133*, 108422.
4. Mallick, J.; Singh, C.K.; AlMesfer, M.K.; Singh, V.P.; Alsubih, M. Groundwater Quality Studies in the Kingdom of Saudi Arabia: Prevalent Research and Management Dimensions. *Water* **2021**, *13*, 1266. [CrossRef]
5. Fallatah, O.; Khattab, M.R. Evaluation of Groundwater Quality and Suitability for Irrigation Purposes and Human Consumption in Saudi Arabia. *Water* **2023**, *15*, 2352. [CrossRef]

6. Truex, M.J.; Pierce, E.M.; Nimmons, M.J.; Mattigod, S.V. *Evaluation of In Situ Grouting as a Potential Remediation Method for the Hanford Central Plateau Deep Vadose Zone, Prepared for the U.S. Department of Energy under Contract DE-AC05-76RL01830*; Pacific Northwest National Laboratory Richland: Washington, DC, USA, 2011; p. 99352.
7. Freitag, P.; Reichenauer, T.G. In situ chemical remediation using the jet grouting technique: A field test. *Environ. Geotech.* **2022**, *11*, 355–365. [CrossRef]
8. Alberti, L.; Angelotti, A.; Antelmi, M.; La Licata, I. A Numerical Study on the Impact of Grouting Material on Borehole Heat Exchangers Performance in Aquifers. *Energies* **2017**, *10*, 703. [CrossRef]
9. Yang, Y.L.; Reddy, K.R.; Zhang, W.J.; Fan, R.D.; Du, Y.J. SHMP-Amended Ca-Bentonite/Sand Backfill Barrier for Containment of Lead Contamination in Groundwater. *Int. J. Environ. Res. Public Health* **2020**, *17*, 370. [CrossRef]
10. Casasso, A.; Salomone, A.; Bianco, C.; Prassede, G.; Sethi, R. A Quantitative Approach to Assessing the Technical and Economic Performance of Source Containment Options for Contaminated Aquifers. *Sustainability* **2021**, *13*, 5346. [CrossRef]
11. Cao, B.; Xu, J.; Wang, F.; Zhang, Y.; O'Connor, D. Vertical Barriers for Land Contamination Containment: A Review. *Int. J. Environ. Res. Public Health* **2021**, *18*, 12643. [CrossRef]
12. Samper, J.; Sobral, B.; Pisani, B.; Naves, A.; Guadaño, J.; Gómez, J.; Fernández, J. Groundwater Flow Model along a Vertical Profile of the Sardas Landfill in Sabiñánigo, Huesca, Spain. *Water* **2023**, *15*, 3457. [CrossRef]
13. Zhou, T.; Hu, J.; Liu, T.; Zhao, F.; Yin, Y.; Guo, M. Engineering Characteristics and Microscopic Mechanism of Soil–Cement–Bentonite (SCB) Cut-Off Wall Backfills with a Fixed Fluidity. *Materials* **2023**, *16*, 4971. [CrossRef] [PubMed]
14. Tatti, F.; Papini, M.; Torretta, V.; Mancini, G.; Boni, M.; Viotti, P. Experimental and numerical evaluation of Groundwater Circulation Wells as a remediation technology for persistent, low permeability contaminant source zones. *J. Contam. Hydrol.* **2019**, *222*, 89–100. [CrossRef] [PubMed]
15. Zhou, N.; Lu, S.; Cai, Y.; Zhao, S. Site Investigation and Remediation of Sulfate-Contaminated Groundwater Using Integrated Hydraulic Capture Techniques. *Water* **2022**, *14*, 2989. [CrossRef]
16. Ciampi, P.; Esposito, C.; Bartsch, E.; Alesi, E.; Papini, M. Pump-and-treat (P&T) vs. groundwater circulation wells (GCW): Which approach delivers more sustainable and effective groundwater remediation? *Environ. Res.* **2023**, *234*, 116538. [CrossRef]
17. Abd-Elaty, I.; Zelenakova, M.; Straface, S.; Vranayová, Z.; Abu-hashim, M. Integrated Modelling for Groundwater Contamination from Polluted Streams Using New Protection Process Techniques. *Water* **2019**, *11*, 2321. [CrossRef]
18. Khalifa, W.M.A.; Achour, B.; Butt, T.; Mirza, C.; Salah, H.; El-Didy, S. The Impact of Injection/Pumping Wells on the Pollution Transport in Groundwater. *Eng. Technol. Appl. Sci. Res.* **2024**, *14*, 12918–12924. [CrossRef]
19. Heejun, S.; Jui-Sheng, C.; Eungyu, P.; Weon, S.; Han, Y.H.K. Numerical evaluation of the performance of injection/extraction well pair operation strategies with temporally variable injection/pumping rates. *J. Hydrol.* **2021**, *598*, 126494, ISSN 0022-1694. [CrossRef]
20. Ahm, H.; Kilanehei, F.; Nazari-Sharabian, M. Impact of Pumping Rate on Contaminant Transport in Groundwater—A Numerical Study. *Hydrology* **2021**, *8*, 103. [CrossRef]
21. Zheng, C.; Wang, P. *MT3DMS: A Modular Three-Dimensional Multispecies Transport Model for Simulation of Advection, Dispersion, and Chemical Reactions of Contaminants in Groundwater Systems*; Documentation and User's Guide; US Army Corps of Engineers Engineer Research and Development Center: Vicksburg, MI, USA, 1999; Contract Report SERDP99-1.
22. Suk, H. Modified Mixed Lagrangian–Eulerian Method Based on Numerical Framework of MT3DMS on Cauchy Boundary. *Groundwater* **2016**, *54*, 508–520. [CrossRef]
23. McDonald, J.M.G.; Harbaugh, A.W. A Modular Three-Dimensional Finite-Difference Ground-Water Flow Model, Reston, VA, USA: U.S. Geological Survey. 1988. Available online: http://pubs.usgs.gov/twri/twri6a1/ (accessed on 24 January 2019).
24. Langevin, C.D.; Hughes, J.D.; Banta, E.; Provost, A.; Niswonger, R.; Panday, S. *MODFLOW 6 Modular Hydrologic Model, Version 6.1.0*; U.S. Geological Survey: Reston, VA, USA, 2019. [CrossRef]
25. Langevin, C.D.; Hughes, J.D.; Banta, E.R.; Niswonger, R.G.; Panday, S.; Provost, A.M. *Documentation for the MODFLOW 6, Groundwater Flow Model: Techniques and Methods 6-A55*; U.S. Geological Survey: Reston, VA, USA, 2017; p. 197. [CrossRef]
26. El Fakharany, M.A.; Monem, M.; Mansour, N. Using Modflow and MT3D Groundwater Flow and Transport Models as a Management Tool for the Quaternary aquifer, East Nile Delta, Egypt. *Int. J. Sci. Commer. Humanit.* **2013**, *1*, 219–223.
27. Bedekar, V.; Morway, E.D.; Langevin, C.D.; Tonkin, M.J. *MT3DUSGS Version 1: A U.S. Geological Survey Release of MT3DMS Updated with New and Expanded Transport Capabilities for Use with MODFLOW, U.S. Geological Survey, 6-A53*; U.S. Geological Survey: Reston, VA, USA, 2016. [CrossRef]
28. Bear, J. *Dynamics of Fluids in Porous Medium*; Elsevier: Amsterdam, The Netherlands, 1972.
29. Bear, J. *Hydraulics of Groundwater*; McGrawHill: New York, NY, USA, 1979.
30. Tsang, C.F.; Buscheck, T.; Doughty, C. Aquifer thermal energy storage: A numerical simulation of Auburn University Field Experiments. *Water Resour. Res.* **1981**, *17*, 647–658. [CrossRef]
31. Van Genuchten, M.T. Analytical solutions for chemical transport with simultaneous adsorption, zero-order production and first-order decay. *J. Hydrol.* **1981**, *49*, 213–233. [CrossRef]
32. Serrano, S.E. Solute transport under non-linear sorption and decay. *Water Res.* **2001**, *35*, 1525–1533. [CrossRef]
33. Guevara Morel, C.R.; van Reeuwijk, M.; Graf, T. Systematic investigation of non-Boussinesq effects in variable-density groundwater flow simulations. *J. Contam. Hydrol.* **2015**, *183*, 82–98. [CrossRef] [PubMed]

34. Khalifa, W.M.A.; El-Didy, S.M.A.; Butt, T.A. Groundwater protection around Makkah sewage treatment plant using hydrological and transport models. *Alex. Eng. J.* **2024**, *109*, 508–519. [CrossRef]
35. IAEA. *Remediation of Sites with Mixed Contamination of Radioactive and Other Hazardous Substances, Technical Reports Series No. 442*; International Atomic Energy Agency: Vienna, Austria, 2006.
36. Zhu, M.; Zhang, Q.; Zhang, X.; Hui, B. Comparative Study of Soil Grouting with Cement Slurry and Cement-Sodium Silicate Slurry. *Adv. Mater. Sci. Eng.* **2018**, *2018*, 1893195. [CrossRef]
37. Ciardi, G.; Vannucchi, G.; Madiai, C. Effects of Colloidal Silica Grouting on Geotechnical Properties of Liquefiable Soils: A Review. *Geotechnics* **2021**, *1*, 460–491. [CrossRef]
38. Zhenkun, H.; Zhanlin, L.; Zejun, H.; Mengxiong, T.; Yupeng, L.; Dingli, S.; Lei, W. Experimental research on the flow law of the grouting fluid in an annular gap between a non-soil-squeezing PHC pipe pile wall and a hole wall. *Front. Ecol. Evol.* **2023**, *11*, 1133631. [CrossRef]
39. Lubo, T.; Xiaobin, C.; Xinxin, Z.; Zhongrong, W.; Yeshun, W.; Kang, X. Numerical analysis and experimental study on slurry diffusion characteristics of vortical oscillatory grouting technology considering soil interface. *Phys. Fluids* **2024**, *36*, 013313. [CrossRef]
40. Zhai, M.; Ma, D.; Bai, H. Diffusion Mechanism of Slurry during Grouting in a Fractured Aquifer: A Case Study in Chensilou Coal Mine, China. *Mathematics* **2022**, *10*, 1345. [CrossRef]
41. Hu, Y.; Liu, W.; Zhen, S.; Gao, K.; Liang, D.; Cheng, S. Diffusion mechanism and sensitivity analysis of slurry while grouting in fractured aquifer with horizontal injection hole. *Carbonates Evaporites* **2020**, *35*, 1–16. [CrossRef]
42. Ngo, I.; Ma, L.; Zhai, J.; Wang, Y.; Wei, T.; Ni, Y. Experimental Investigation of CO2-Induced Silica Gel as the Water Blocking Grout Effect of Aquifer Ions. *ACS Omega* **2022**, *30*, 27090–27101. [CrossRef] [PubMed] [PubMed Central]
43. David, L. Grouting—For Groundwater Control and Mitigation Of Ground Movements. In *AGS SANT Symposium 2019–Tunnelling Under Adelaide*; AT Publishing: Adelaide, SA, Australia, 2019.
44. Shucai, L.; Rentai, L.; Qingsong, Z.; Xiao, Z. Protection against water or mud inrush in tunnels by grouting: A review. *J. Rock Mech. Geotech. Eng.* **2016**, *8*, 753–766, ISSN 1674-7755. [CrossRef]
45. Jin-Quan, L.; Wei-Zhong, C.; Ka-Veng, Y.; Xiao-Sheng, Z. Groundwater-mud control and safety thickness of curtain grouting for the Junchang Tunnel: A case study. *Tunn. Undergr. Space Technol.* **2020**, *103*, 103429, ISSN 0886-7798. [CrossRef]
46. Lokesh, P.P.; Prashant, S.; Tahereh, J.; Shiv, B.; Deyi, H.; Sabry, M.S.; Jörg, R.; David, O.; Dane, L.; Hailong, W.; et al. Contaminant containment for sustainable remediation of persistent contaminants in soil and groundwater. *J. Hazard. Mater.* **2023**, *455*, 131575, ISSN 0304-3894. [CrossRef]
47. Zhipeng, D.; Jiajun, C.; Shengnan, K.; Qi, X.; Zhenquan, W. Experimental investigations on spreading and displacement of fluid plumes around an injection well in a contaminated aquifer. *J. Hydrol.* **2023**, *617*, 129062, ISSN 0022-1694. [CrossRef]
48. Poursalehi, F.; Akbarpour, A.; Hashemi, S.R. Simulating the effect of injection well on groundwater table in unconfined aquifer using numerical model of Isogeometric analysis and optimization of injection rate with PSO algorithm. *Q. J. Eng. Geol. Hydrogeol.* **2022**, *55*, qjegh2021-117. [CrossRef]
49. Huang, Y.; Li, Y.; Knappett, P.S.K.; Montiel, D.; Wang, J.; Aviles, M.; Hernandez, H.; Mendoza-Sanchez, I.; Loza-Aguirre, I. Water Quality Assessment Bias Associated with Long-Screened Wells Screened across Aquifers with High Nitrate and Arsenic Concentrations. *Int. J. Environ. Res. Public Health* **2022**, *11*, 9907. [CrossRef] [PubMed] [PubMed Central]
50. Mostafa, M.M.; Helal, E.Y.; Sobeh, M.F.; Abdelhaleem, F.S. EFFECT of Dewatering System on Groundwater Contaminations Transport, ERJ, PART 4. *Civil Eng.* **2023**, *46*, 353–364.